

NeoNeXt: Novel neural network operator and architecture based on the patch-wise matrix multiplications

Vladimir Korviakov¹ and Denis Kopusov¹

Moscow Media Technology lab, Huawei Technologies Co., Ltd
korviakov.vladimir1,kopusov.denis1@huawei.com
<https://www.huawei.com/>

Abstract. Most of the computer vision architectures nowadays are built upon the well-known foundation operations: fully-connected layers, convolutions and multi-head self-attention blocks. In this paper we propose a novel foundation operation - NeoCell - which learns matrix patterns and performs patchwise matrix multiplications with the input data. The main advantages of the proposed operator are (1) simple implementation without need in operations like *im2col*, (2) low computational complexity (especially for large matrices) and (3) simple and flexible implementation of up-/down-sampling. We validate NeoNeXt family of models based on this operation on ImageNet-1K classification task and show that they achieve competitive quality.

Keywords: Neural Network architecture · Computer Vision

1 Introduction

A plethora of the specialized AI hardware such as Neural Processing Units (NPUs) have appeared recently. These devices are typically good at running parallelizable tasks of tensor and matrix multiplications and additions, however they also set specific limitations for the models to be deployed. For example, NPUs provide fast vector instructions and very efficient large matrix multiplications, but the memory operations are relatively slow. Non-vectorizable operations or dynamic model structure should also be avoided.

Thus, it is important to explore new basic paradigms of the Neural Networks, which can utilize the advantages of NPUs and avoid their disadvantages, while keeping the quality of the solution of the target problem.

In this paper we continue this exploration by considering Huawei Ascend [11] based on Da Vinci architecture [19] as our target platform. This device has been designed to maximize the efficiency of the most popular neural architectures at the moment of design, such as ResNet [9]. These architectures are based on the convolution operation that can be computed in several ways. The most popular algorithm is to transform the input data of shape $C_{in} \times H_{in} \times W_{in}$ to the matrix of size $H_{in}W_{in} \times C_{in}K^2$ using *im2col* operation [3]. This matrix is then multiplied by the matrix of shape $C_{in}K^2 \times C_{out}$ obtained from the convolutional weights by reshaping them. Practically, *im2col* operation increases the size of input data by K^2 times, where K is the size of kernel (square kernel is considered for simplicity).

To solve the aforementioned problems of the convolution we propose a novel operation - **NeoCell** - that is built upon a sequence of matrix multiplications in a way that differs from all known architectures existing today. We also construct a family of architectures called **NeoNeXt** based on the ConvNeXt [21], while using this newly designed operation instead of 2D convolutional layers. NeoCell essentially multiplies the input by two matrices of weights from the left side and from the right side.

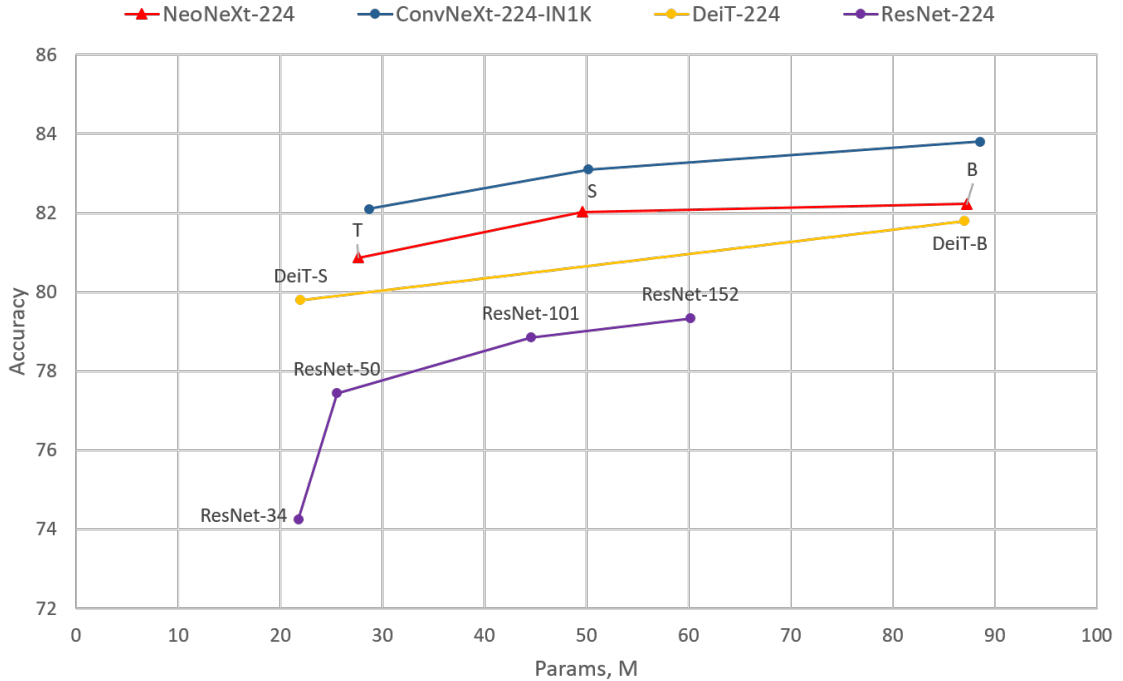


Fig. 1: **ImageNet-1K accuracy vs parameters**. NeoNeXt is compared to ResNet, DeiT and ConvNeXt. Although we do not achieve state-of-the-art performance, we prove that NeoCell operation is a viable choice. It’s also shown that NeoNeXt quality grows with the number of parameters, which means that models are scalable. **IN1K** means that ConvNeXt was not pretrained on external data such as ImageNet-22K.

The most straightforward application for this operator is to replace the depthwise convolution, which is inferior in several aspects. First of all, NeoCell is $2/K$ times less complex (see Section 3.6), where K is the convolutional kernel size and NeoCell matrix size. Secondly, it does not require im2col and allows to reduce the amount of memory required by the intermediate representations. NeoCell also allows to do flexible data subsampling with a fractional scaling factor, which is described in Section 3.2. Finally, implementation of NeoCell is essentially a series of two multiplications by the large structured matrices, which is very efficient and can be done on any device.

We test our family of the models on the ImageNet classification task and achieve the performance competitive to the modern architectures. The details of the experiments are provided in Section 4.1.

2 Related Work

A lot of vendors have recently addressed the problem of AI cost minimization by designing specialized AI acceleration hardware and platforms. The examples of such platforms are Google Cloud TPU [8,14], Nvidia Jetson [23], Huawei Ascend [11], Intel Movidius Myriad [12] and etc.

Typical way to minimize the latency and maximize the throughput is to design specialized low-level kernels for existing operators. FlashAttention [6] and FlashAttention-2 [5] are good examples of such operators.

The classical convolutional operator optimizations are based on Winograd method [31,17], im2col method [3] or Fast Fourier Transform and Convolution Theorem [22].

Algorithmic optimizations can have one big benefit: they can be exactly or approximately equivalent to non-optimized methods, thus existing pretrained models can be accelerated without training from scratch. The disadvantage of algorithmic optimizations is that the designed operators are limited by the theoretical properties of the baseline method. Thus it is important to explore novel fundamental algorithms that allow to outperform existing methods.

One of the previous attempts to optimize convolutions for specialized devices was depthwise separable convolution mostly known from the MobileNet and EfficientNet families of models. The usual convolution is replaced by two convolutional layers: spatial (acts on each channel separately) and pointwise (has a kernel of size 1). It allows to reduce the amount of memory consumed by the model parameters and make it less computationally complex without any effects on the quality. However, the problem of intermediate representation size during im2col stays.

One more possible way to increase the efficiency of the hardware utilization is to design hardware-friendly neural architectures using Neural Architecture Search methods [27,18,2]. The disadvantage of NAS-based methods is that only limited set of already designed operators can be included into the search space.

Another notable example of the novel architecture paradigm is MLP-Mixer architecture [29] that builds a competitive model based exclusively on multi-layer perceptrons (MLPs).

3 Method

3.1 NeoCell Operator

The key idea of the proposed operator ("NeoCell") is the following: given the input data tensor X of shape $[C \times H \times W]$ (batch dimension is omitted for simplicity) we define two trainable weight tensors: L of shape $[C \times h' \times h]$ and R of shape $[C \times w \times w']$. These tensors can be considered as C matrices of shape $[h' \times h]$ and $[w \times w']$ correspondingly. Then input can be reshaped to shape $[C \times \frac{H}{h} \times h \times \frac{W}{w} \times w]$ and permuted to shape $[C \times \frac{H}{h} \times \frac{W}{w} \times h \times w]$ (Fig. 2). Then the output can be computed as

$$Y_{c,i,j} = L_c X_{c,i,j} R_c, \quad (1)$$

$$c \in [1, \dots, C], i \in [1, \dots, \frac{H}{h}], j \in [1, \dots, \frac{W}{w}]$$

In other words, for each channel c we split data into $\frac{H}{h} \cdot \frac{W}{w}$ patches of shape $[h \times w]$ and each of them multiplied by matrices L_c (left side multiplication) and R_c (right side multiplication). Optionally, trainable bias B of shape $[C \times h' \times w']$ can be added to the result. The output has shape $[C \times \frac{H}{h} \times \frac{W}{w} \times h' \times w']$ which is permuted to $[C \times \frac{H}{h} \times h' \times \frac{W}{w} \times w']$ and reshaped to $[C \times \frac{H}{h} \cdot h' \times \frac{W}{w} \cdot w']$.

The proposed operation together with the other common operations like activation functions, normalization, fully-connected layers (or pointwise convolutions) and skip connection allows to construct the neural of the stage structure: down-sampling of the data is allowed between the stages,

while within each stage spatial shape of the data is not changed. In Section 3.4 we show mathematically equivalent formulation of the NeoCell operator without need in reshape and permute operations.

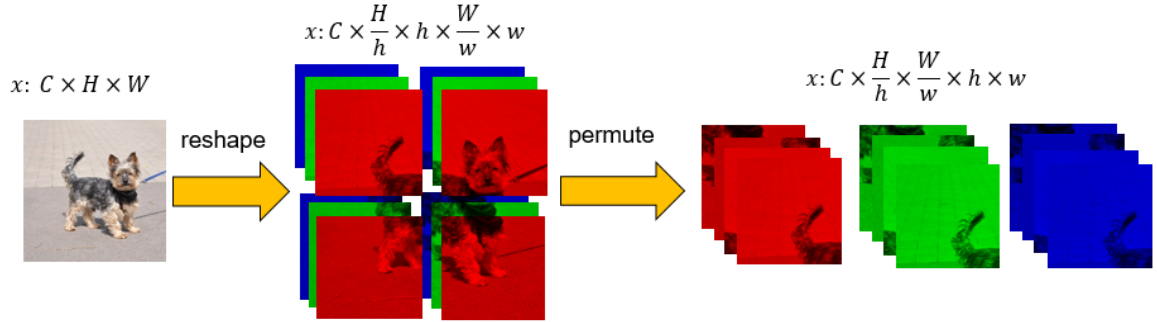


Fig. 2: Illustration of splitting of the data into the patches

3.2 Up- and Down-sampling

Obviously, if weight matrices are square, i.e. $h' = h$ and $w' = w$, then the shape of input and output data are the same. If $h' < h$ and/or $w' < w$ then NeoCell performs down-sampling of the input data by one or both of the spatial dimensions. If $h' > h$ and/or $w' > w$ then NeoCell performs up-sampling of the input data by one or both of the spatial dimensions. This property enables flexible change of the data spatial size. The simple illustrations of up- and down-sampling are shown on Fig. 3a and Fig. 3b correspondingly.

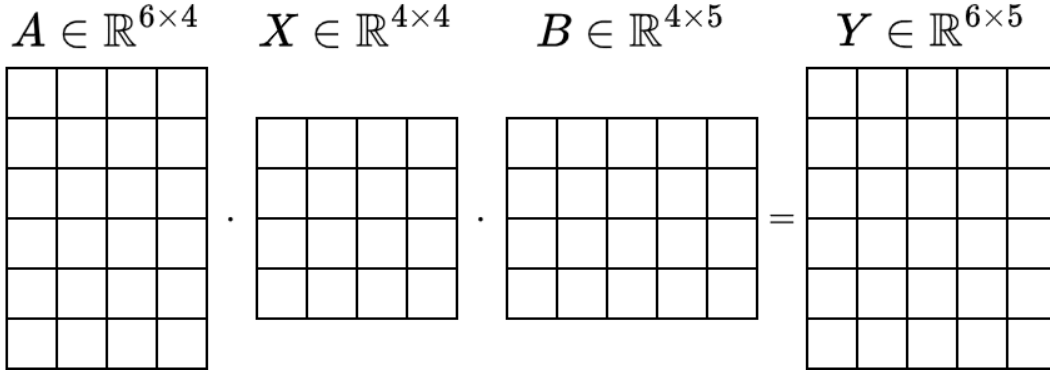
3.3 Inter-channel Information Exchange

Conceptually, NeoCell can be considered as a replacement of depthwise convolution. It means that single NeoCell operation connects each c -th input channel to the corresponding output channel, and there is no information exchange between different channels. To enable the information exchange between the channels we utilize pointwise convolutions (or fully-connected layers applied to the channel dimension). This approach used in a number of modern architectures like MobileNet [10] and EfficientNet [28].

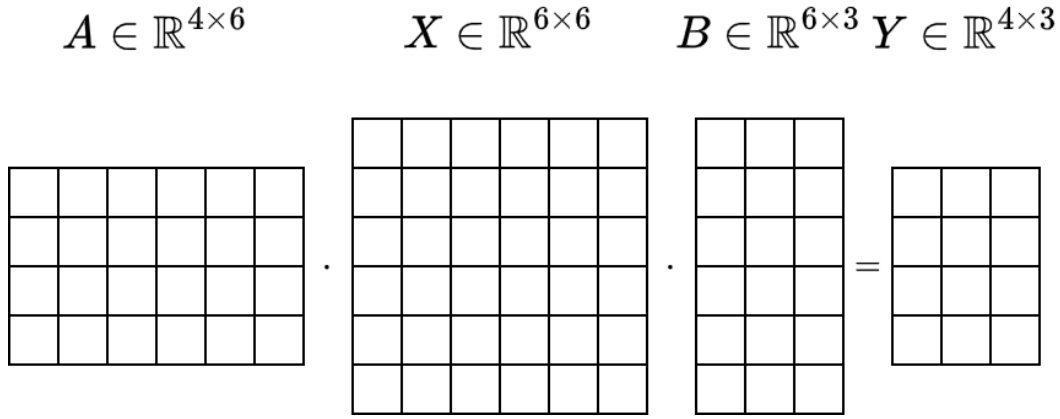
3.4 Block-diagonal Implementation

In practice it may be inefficient to permute the data and multiply matrices of small size. Modern device like Huawei Ascend [11] operate with larger matrices with higher efficiency. However, it may be hard to train model with large weight filters and special tricks should be applied [7,20].

To overcome this contradiction we propose to reformulate the NeoCell operation in terms of the block-diagonal matrix multiplication. In this case, the data X is kept in the original format $[C \times H \times W]$ but interpreted as block matrix, where blocks X_{ij} correspond to the patches in the



(a) Using NeoCell operator for up-sampling



(b) Using NeoCell operator for down-sampling

Fig. 3: Methods of spatial size change

original formulation. Left and right matrices A_c and B_c of channel $c \in [1..C]$ are constructed as block-diagonal matrices with the original matrices used as the shared blocks.

$$\mathbf{A}_c = \begin{bmatrix} \mathbf{L}_c & \mathbf{0} & \cdots & \mathbf{0} \\ \mathbf{0} & \mathbf{L}_c & \cdots & \mathbf{0} \\ \vdots & \vdots & \ddots & \vdots \\ \mathbf{0} & \cdots & \mathbf{0} & \mathbf{L}_c \end{bmatrix}; \quad \mathbf{B}_c = \begin{bmatrix} \mathbf{R}_c & \mathbf{0} & \cdots & \mathbf{0} \\ \mathbf{0} & \mathbf{R}_c & \cdots & \mathbf{0} \\ \vdots & \vdots & \ddots & \vdots \\ \mathbf{0} & \cdots & \mathbf{0} & \mathbf{R}_c \end{bmatrix} \quad (2)$$

Now the output data can be computed as $Y_c = A_c X_c B_c$ for each $c \in [1..C]$. The simplest example of this idea is shown in the Eq. (3). The input data is split into four virtual patches, without actual change of the shape. This formulation allows to better utilize AI acceleration devices. In our experiments this idea allowed to accelerate the implementation 15 times on NVidia V100

GPU and PyTorch framework. Additional acceleration can be achieved using specialized low-level sparse matrix multiplication operators.

$$Y_c = A_c X_c B_c = \begin{bmatrix} \mathbf{L}_c & \mathbf{0} \\ \mathbf{0} & \mathbf{L}_c \end{bmatrix} \begin{bmatrix} \mathbf{X}_{c11} & \mathbf{X}_{c12} \\ \mathbf{X}_{c21} & \mathbf{X}_{c22} \end{bmatrix} \begin{bmatrix} \mathbf{R}_c & \mathbf{0} \\ \mathbf{0} & \mathbf{R}_c \end{bmatrix} = \begin{bmatrix} \mathbf{L}_c \mathbf{X}_{c11} \mathbf{R}_c & \mathbf{L}_c \mathbf{X}_{c12} \mathbf{R}_c \\ \mathbf{L}_c \mathbf{X}_{c21} \mathbf{R}_c & \mathbf{L}_c \mathbf{X}_{c22} \mathbf{R}_c \end{bmatrix} \quad (3)$$

3.5 Inter-patch Information Exchange

Unlike regular convolutions, within a stage NeoCell has constant receptive field which is equal to the patch size, even for a single layer. The receptive field does not increase for the deeper layers. Pointwise convolutions do not solve this problem, because they also do not increase the receptive field. To address this problem two different solutions are proposed:

1. Construct block-diagonal NeoCell with different matrix sizes for different channels (Fig. 4a). For example, first group of channels uses matrix 2x2, second group – 3x3, etc.
2. Construct block-diagonal NeoCell with spatially shifted matrices for different channels (Fig. 4b). For example, all channels use matrix 3x3, and in the first group of channels matrices are not shifted, in the second group – shifted by 1 pixel by width and height dimension, in the third group – shifted by 2 pixels. Instead of zeroing, the upper-left and lower-right corners of block-diagonal matrix can be filled with corresponding lower-right and upper-left parts of the weight matrix.

These ideas can be combined together: all channels can be split into several groups with different matrix sizes, and each group can be split into n_i subgroups with incrementally growing spatial shift (n_i is matrix size for the i -th group). Together with the pointwise convolutions proposed ideas lead to information exchange between the adjacent regions of the data, thus receptive field grows with the depth of the network.

3.6 Complexity analysis

Consider input tensor of shape $[C \times H \times W]$, depthwise convolution with kernel $[k \times k]$ and NeoCell with both left and right weight matrices of size $[k \times k]$ (no bias in both cases). Then, the complexity of depthwise convolution (in terms of number of multiplication operations) is

$$T_{DWC} = C \cdot H \cdot W \cdot k^2 \quad (4)$$

Assuming the naïve matrix multiplication algorithm with $\mathcal{O}(n^3)$ complexity, the complexity of NeoCell is

$$T_{NEO} = 2 \cdot C \cdot \frac{H}{k} \cdot \frac{W}{k} \cdot k^3 = 2 \cdot C \cdot H \cdot W \cdot k \quad (5)$$

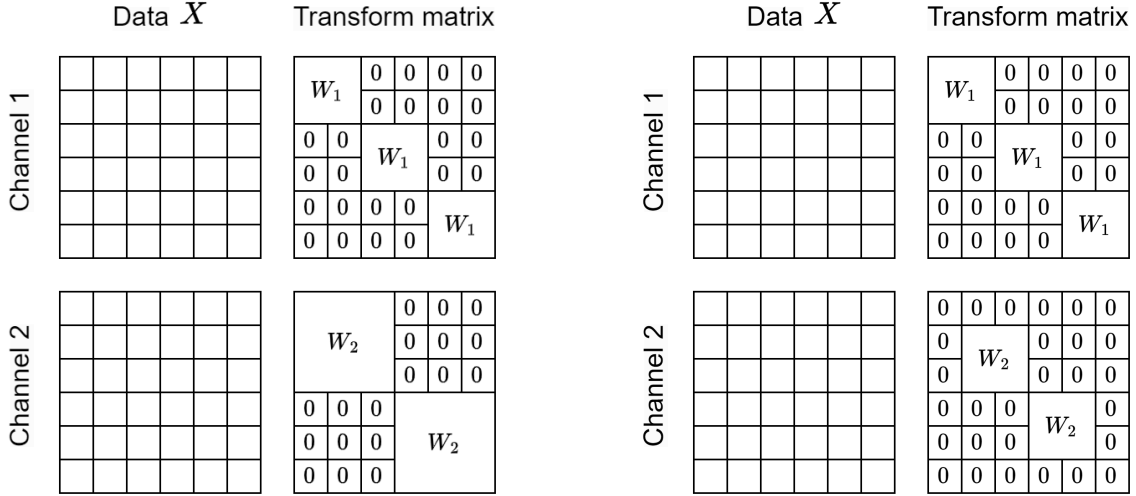
Thus $T_{NEO} < T_{DWC}$ if $k > 2$.

As an additional advantage, NeoCell operator doesn't need extra memory operation on the input data such as `im2col` [3] which may be important in certain cases.

3.7 Initialization method

We have found that proper initialization method is very important for the final quality of the model. We use Line 22 to initialize each NeoCell matrix.

Every NeoCell square matrix is initialized as an identity matrix. Non-square matrices are initialized as "skewed" identity matrices, i.e. behave as average pooling in the local region defined by



(a) Using different matrix sizes for different channels

(b) Using spatially shifted matrices for different channels

Fig. 4: Methods of inter-patch information exchange. Only right NeoCell matrices are shown here.

ratio between input and output size. Additionally, Gaussian noise $\mathcal{N}(0, \frac{1}{\sqrt{w \cdot h}})$ is added to every element of both square and non-square matrices. Further we call the proposed initialization method "NeoInit". We investigate this method in Section 4.2.

4 NeoNeXt architecture

In our architecture design we follow the scheme proposed by [21], including the block structure, depth, width and resolution. The key differences between ConvNeXt and our architecture ("NeoNeXt") are:

- In the stem we use Space-To-Depth with patch size 4 which decreases width and height 4 times and increases channels number 16 times (from 3 to 48). Then pointwise convolution increases channels number to 96. After that Batch Normalization [13] is applied.
- In model blocks we use NeoCell operator instead of the depthwise convolutions. In the stages 1 to 3 of the model we split all channels into two equal parts and use matrices 4x4 in the first part and 7x7 in the second part. In both parts we enable spatial shifts of the matrices (see Section 3.5). In the stage 4 we use 7x7 matrices in all channels without spatial shift (as the data spatial size is already small enough and there is no need in cross-patch exchange).
- Instead of the Layer Normalization [1] in NeoNeXt we prefer to use Batch Normalization [13] because it can be efficiently fused with the previous linear operation (convolution or NeoCell) and requires no extra operations during the inference which is beneficial for the deployment.
- For the down-sampling between the stages and to change the width from C_i to C_{i+1} we use the following sequence of operations:

$NeoCell(h = 2, h' = 1, w = 2, w' = 1) \rightarrow$
 $BatchNorm \rightarrow GELU \rightarrow$
 $PointwiseConv(C_i, C_{i+1}) \rightarrow BatchNorm \rightarrow GELU.$

0.55	-0.02	-0.02	-0.03	1.03	-0.01	-0.01	-0.02	0.02	-0.05	0.04
0.53	-0.07	0.05	-0.02	-0.02	1.01	-0.01	0.03	-0.04	-0.01	-0.01
0.01	0.49	0.05	-0.06	0.02	-0.02	1.00	-0.02	0.00	0.01	-0.02
-0.01	0.49	0.04	-0.03	0.02	0.02	0.01	1.02	-0.01	-0.00	-0.02
-0.01	-0.03	0.50	0.02	-0.01	0.01	-0.01	-0.01	0.99	-0.02	-0.01
-0.03	0.04	0.53	0.02	-0.00	-0.02	0.00	0.03	0.02	1.00	-0.02
0.03	-0.02	-0.00	0.47	-0.02	0.03	0.00	-0.01	0.00	0.04	1.00
-0.01	0.02	-0.02	0.49	-0.02	0.03	0.00	-0.01	0.00	0.04	1.00

(a) 8×4 matrix

(b) 7×7 matrix

0.59	0.47	-0.03	-0.06	0.05	-0.13
0.10	-0.04	0.52	0.49	0.08	-0.11
-0.02	-0.02	0.06	-0.06	0.49	0.45

(c) 3×6 matrix

Fig. 5: Examples of NeoInit method for different matrices

Algorithm 1: NeoCell initialization algorithm

Data: Height: $h > 0$, Width: $w > 0$
Result: Initialization matrix $W_0 \in \mathbb{R}^{h \times w}$

```

1 /* Initialize with zero matrix */
2  $W_0 \leftarrow 0_{h \times w}$ ;
3 if  $h < w$  then
4    $step \leftarrow \text{round}(w/h)$ ;
5   for  $i \leftarrow 0$  to  $h - 1$  do
6      $start \leftarrow i \cdot step$ ;
7      $end \leftarrow \min((i + 1) \cdot step, w)$ ;
8     for  $j \leftarrow start$  to  $end$  do
9        $W_0[i, j] \leftarrow \frac{1}{end - start}$ ;
10 else if  $h > w$  then
11    $step \leftarrow \text{round}(h/w)$ ;
12   for  $i \leftarrow 0$  to  $w - 1$  do
13      $start \leftarrow i \cdot step$ ;
14      $end \leftarrow \min((i + 1) \cdot step, h)$ ;
15     for  $j \leftarrow start$  to  $end$  do
16        $W_0[j, i] \leftarrow \frac{1}{end - start}$ ;
17 else
18   /* Square matrix, identity */
19    $W_0 \leftarrow I_h$ ;
20 /* Add Gaussian noise */
21  $W_0 \leftarrow W_0 + \mathcal{N}_{h \times w}(0, \frac{1}{\sqrt{w \cdot h}})$ ;
22 return  $W_0$ 

```

4.1 ImageNet-1K experiments

In this section we evaluate our NeoNeXt family of models with NeoCell operation on well-known ImageNet-1K [25] image classification benchmark. We mostly follow the training recipe from ConvNeXt paper [21]. We run our models for 300 epochs, including 20 epochs of linear learning rate warmup. We use AdamW optimizer with $\beta_1 = 0.9$ and $\beta_2 = 0.999$. As for the regularization techniques we apply weight decay of 0.05, label smoothing of 0.1, randaugment [4], mixup [34], cutmix [33] and random erasing. We also tried exponential moving average (EMA) [24], but it did not improve the accuracy. The details can be found in Table 2.

We have trained three models of different size, namely, NeoNeXt-T/S/B with 28M/50M/87M parameters, correspondingly, and compared them to the previously known classification models. We show that NeoNeXt models demonstrate competitive performance (Table 1) with the best model achieving 82.23% top-1 accuracy at resolution 224 and 83.32% at resolution 384. While we do not achieve state-of-the-art performance, we prove that NeoCell operator works as intended and serves a good replacement for depth-wise convolutions. We also show that NeoNeXt models scale both with model size and image resolution. Moreover, NeoNext models are more efficient than ConvNeXt with respect to FLOPs according to Table 1, but this effect is not very significant due to small share of depth-wise convs in the total number of model’s FLOPs.

Table 1: **Classification results on ImageNet-1K dataset.** We compare with several well-known models with comparable number of parameters and FLOPs. NeoNeXt does not beat SoTA, but achieves comparable results, which proves its viability.

Model	res	# params	GFLOPs	Top-1
DeiT-S [30]	224	22M	4.60	79.8
NeoNeXt-T	224	27.7M	4.40	80.87
ConvNeXt-T	224	28.7M	4.50	82.10
NeoNeXt-S	224	49.6M	8.60	82.03
ConvNeXt-S	224	50.2M	8.70	83.10
DeiT-B [30]	224	87M	17.6	81.8
NeoNeXt-B	224	87.3M	15.19	82.23
ConvNeXt-B	224	88.6M	15.4	83.80
NeoNeXt-T	384	27.7M	13.27	81.36
NeoNeXt-S	384	49.6M	25.71	83.32
NeoNeXt-B	384	87.3M	45.21	83.11

4.2 Ablation Study of NeoCell Initialization

To investigate the impact of the NeoInit method we made experiments on the CIFAR-10 dataset [16]. We train NeoNeXt-T model for 25 epochs with SGD optimizer with momentum 0.9, batch size 64. During the first epoch we use linear learning rate warmup to the maximum value 0.1, then cosine annealing schedule is applied.

Fig. 6 and Table 3 show the comparison of the proposed NeoInit initialization method (see Section 3.7) with the baseline random normal initialization of the NeoCell matrices (without the identity matrix): $L_0 = \mathcal{N}(0, \frac{1}{\sqrt{h}})$ and $R_0 = \mathcal{N}(0, \frac{1}{\sqrt{w}})$. Each curve is averaged over 5 runs with different random seeds.

Experimental results show that the proposed initialization method allows to avoid overfitting and improve final validation accuracy of the model by 3.8 percentage points.

Interesting that with random normal initialization (i.e. without NeoInit method) approximately 75% of the experiments diverged. In contrast, all NeoInit experiments converged well with the same settings. This indicates positive impact of the NeoInit method to the training convergence stability.

5 Discussion and Future Work

Many interesting research directions are left outside the scope of this paper. The following directions can be considered for the future work:

1. Theoretical study of the NeoCell properties, such as generalization ability, convergence, analysis of the learned matrix patterns *etc.*;
2. Design of the optimized low-level operators to better utilize hardware capabilities. We did our proof-of-concept experiments in PyTorch framework using Python API. Then we made NeoCell implementation using C++ API, which led to about 3 times acceleration. Still, we think that low-level optimization can significantly accelerate both training and inference;
3. Search of better architecture and adaptation of the NeoCell-based architecture to the specialized NPU hardware similarly to [28] or [18]. Currently, the main computational bottleneck in the current architecture is not NeoCell operators, but pointwise convolutions. Generalization to 3D

Table 2: ImageNet-1K training parameters

hyperparameters	NeoNeXt-T/S/B
	ImageNet-1K 224 ² / 384 ²
weight init	neoinit
optimizer	AdamW
base LR	4e-3/4e-3/2e-3
weight decay	0.05
momentum	(0.9, 0.999)
batch size	4096/4096/2048
epochs	300
LR schedule	cosine
warmup epochs	20
warmup schedule	linear
randaugment	n=2, m=9
mixup	0.8
cutmix	1.0
random erasing	0.25
label smoothing	0.1
drop path	0.1/0.4/0.5
gradient clip	None
EMA decay	None

case can be studied, i.e. similar to non depthwise convolution, where filter is applied to the group of or all input channels;

4. Application of the modern training tricks to maximize the model quality, including masked autoencoders paradigm [32] and use of large pre-training datasets [15].
5. Investigation of the new applications, where NeoCell can be beneficial. This includes both classical computer vision problems such as detection or segmentation and modern multi-modal directions like text-to-image retrieval and generation of images and videos.
6. Use of continuous weights representation instead of discrete, similar to [26].
7. Use of fast matrix multiplication algorithms to compute NeoCell operator kernel. It may allow to further decrease the complexity and even make it sub-linear with respect to the NeoCell matrix size according to Eq. (5).

6 Conclusions

NeoCell operation can be considered as a replacement of depthwise convolutions having less computational complexity. Our experiments show that the architectures built using NeoCell show good performance on computer vision problems. Although our models don't outperform state-of-the-art, we are convinced that the proposed method has high potential due to its simplicity and flexibility and can become a foundation for the new architectures. Simple and efficient design of the proposed operation enable further improvement based on decompositions, special parameterization and well-studied linear algebra theory.

Table 3: NeoInit ablation study, CIFAR-10 dataset. Results are averaged over 5 runs with different random seeds.

Model	Init method	Validation loss	Validation accuracy, %
NeoNeXt-T	Random normal	0.573	84.65
NeoNeXt-T	NeoInit	0.390 (-0.183)	88.45 (+3.8)

References

1. Ba, J.L., Kiros, J.R., Hinton, G.E.: Layer normalization (2016). <https://doi.org/10.48550/ARXIV.1607.06450>, <https://arxiv.org/abs/1607.06450>
2. Baymurzina, D., Golikov, E., Burtsev, M.: A review of neural architecture search. *Neurocomputing* **474**, 82–93 (2022). <https://doi.org/https://doi.org/10.1016/j.neucom.2021.12.014>, <https://www.sciencedirect.com/science/article/pii/S0925231221018439>
3. Chellapilla, K., Puri, S., Simard, P.Y.: High performance convolutional neural networks for document processing (2006), <https://api.semanticscholar.org/CorpusID:14936779>
4. Cubuk, E.D., Zoph, B., Shlens, J., Le, Q.V.: Randaugment: Practical automated data augmentation with a reduced search space. In: *Proceedings of the IEEE/CVF conference on computer vision and pattern recognition workshops*. pp. 702–703 (2020)
5. Dao, T.: Flashattention-2: Faster attention with better parallelism and work partitioning (2023)
6. Dao, T., Fu, D., Ermon, S., Rudra, A., Ré, C.: Flashattention: Fast and memory-efficient exact attention with io-awareness. In: Koyejo, S., Mohamed, S., Agarwal, A., Belgrave, D., Cho, K., Oh, A. (eds.) *Advances in Neural Information Processing Systems*. vol. 35, pp. 16344–16359. Curran Associates, Inc. (2022), https://proceedings.neurips.cc/paper_files/paper/2022/file/67d57c32e20fd0a7a302cb81d36e40d5-Paper-Conference.pdf
7. Ding, X., Zhang, X., Zhou, Y., Han, J., Ding, G., Sun, J.: Scaling up your kernels to 31x31: Revisiting large kernel design in cnns (2022). <https://doi.org/10.48550/ARXIV.2203.06717>, <https://arxiv.org/abs/2203.06717>
8. Google: Edge TPU (2019), <https://cloud.google.com/edge-tpu/>
9. He, K., Zhang, X., Ren, S., Sun, J.: Deep residual learning for image recognition. In: *CVPR* (2016)
10. Howard, A.G., Zhu, M., Chen, B., Kalenichenko, D., Wang, W., Weyand, T., Andreetto, M., Adam, H.: MobileNets: Efficient convolutional neural networks for mobile vision applications. *arXiv:1704.04861* (2017)
11. Huawei: Ascend Computing (2024), <https://e.huawei.com/en/products/computing/ascend>
12. Intel: Intel Movidius Myriad™ X Vision Processing Unit (2021), <https://www.intel.com/content/www/us/en/products/details/processors/movidius-vpu/movidius-myriad-x.html>
13. Ioffe, S., Szegedy, C.: Batch normalization: Accelerating deep network training by reducing internal covariate shift (2015). <https://doi.org/10.48550/ARXIV.1502.03167>, <https://arxiv.org/abs/1502.03167>
14. Jouppi, N.P., Young, C., Patil, N., Patterson, D.: A domain-specific architecture for deep neural networks. *Commun. ACM* **61**(9), 50–59 (Aug 2018). <https://doi.org/10.1145/3154484>, <https://doi.org/10.1145/3154484>
15. Kolesnikov, A., Beyer, L., Zhai, X., Puigcerver, J., Yung, J., Gelly, S., Houlsby, N.: Big transfer (bit): General visual representation learning. In: *Computer Vision—ECCV 2020: 16th European Conference, Glasgow, UK, August 23–28, 2020, Proceedings, Part V* 16. pp. 491–507. Springer (2020)
16. Krizhevsky, A., Hinton, G., et al.: Learning multiple layers of features from tiny images (2009)
17. Lavin, A., Gray, S.: Fast algorithms for convolutional neural networks. 2016 *IEEE Conference on Computer Vision and Pattern Recognition (CVPR)* pp. 4013–4021 (2015), <https://api.semanticscholar.org/CorpusID:962822>
18. Letunovskiy, A., Korviakov, V., Polovnikov, V., Kargapol'tseva, A., Mazurenko, I., Xiong, Y.: Isynet: Convolutional neural networks design for ai accelerator (2022)

19. Liao, H., Tu, J., Xia, J., Zhou, X.: Davinci: A scalable architecture for neural network computing. In: Hot Chips Symposium. pp. 1–44 (2019)
20. Liu, S., Chen, T., Chen, X., Chen, X., Xiao, Q., Wu, B., Pechenizkiy, M., Mocanu, D., Wang, Z.: More convnets in the 2020s: Scaling up kernels beyond 51x51 using sparsity (2022). <https://doi.org/10.48550/ARXIV.2207.03620>, <https://arxiv.org/abs/2207.03620>
21. Liu, Z., Mao, H., Wu, C.Y., Feichtenhofer, C., Darrell, T., Xie, S.: A convnet for the 2020s. Proceedings of the IEEE/CVF Conference on Computer Vision and Pattern Recognition (CVPR) (2022)
22. Mathieu, M., Henaff, M., LeCun, Y.: Fast training of convolutional networks through ffts. CoRR [abs/1312.5851](https://arxiv.org/abs/1312.5851) (2013), <https://api.semanticscholar.org/CorpusID:18233038>
23. NVidia: Embedded Systems for Next-Generation Autonomous Machines (2021), <https://www.nvidia.com/en-gb/autonomous-machines/embedded-systems/>
24. Polyak, B.T., Juditsky, A.B.: Acceleration of stochastic approximation by averaging. SIAM journal on control and optimization **30**(4), 838–855 (1992)
25. Russakovsky, O., Deng, J., Su, H., Krause, J., Satheesh, S., Ma, S., Huang, Z., Karpathy, A., Khosla, A., Bernstein, M., Berg, A.C., Fei-Fei, L.: ImageNet Large Scale Visual Recognition Challenge. International Journal of Computer Vision (IJCV) **115**(3), 211–252 (2015). <https://doi.org/10.1007/s11263-015-0816-y>
26. Solodskikh, K., Kurbanov, A., Aydarkhanov, R., Zhelavskaya, I., Parfenov, Y., Song, D., Lefkimmatis, S.: Integral neural networks. In: Proceedings of the IEEE/CVF Conference on Computer Vision and Pattern Recognition (CVPR). pp. 16113–16122 (June 2023)
27. Tan, M., Chen, B., Pang, R., Vasudevan, V., Sandler, M., Howard, A., Le, Q.V.: Mnasnet: Platform-aware neural architecture search for mobile (2019)
28. Tan, M., Le, Q.: Efficientnet: Rethinking model scaling for convolutional neural networks. In: ICML (2019)
29. Tolstikhin, I.O., Houlsby, N., Kolesnikov, A., Beyer, L., Zhai, X., Unterthiner, T., Yung, J., Steiner, A., Keysers, D., Uszkoreit, J., Lucic, M., Dosovitskiy, A.: Mlp-mixer: An all-mlp architecture for vision. In: Ranzato, M., Beygelzimer, A., Dauphin, Y., Liang, P., Vaughan, J.W. (eds.) Advances in Neural Information Processing Systems. vol. 34, pp. 24261–24272. Curran Associates, Inc. (2021), https://proceedings.neurips.cc/paper_files/paper/2021/file/cba0a4ee5ccd02fda0fe3f9a3e7b89fe-Paper.pdf
30. Touvron, H., Cord, M., Douze, M., Massa, F., Sablayrolles, A., Jegou, H.: Training data-efficient image transformers and distillation through attention. In: International Conference on Machine Learning. vol. 139, pp. 10347–10357 (July 2021)
31. Winograd, S.: Arithmetic Complexity of Computations. Society for Industrial and Applied Mathematics (1980). <https://doi.org/10.1137/1.9781611970364>, <https://epubs.siam.org/doi/abs/10.1137/1.9781611970364>
32. Woo, S., Debnath, S., Hu, R., Chen, X., Liu, Z., Kweon, I.S., Xie, S.: Convnext v2: Co-designing and scaling convnets with masked autoencoders. In: Proceedings of the IEEE/CVF Conference on Computer Vision and Pattern Recognition (CVPR). pp. 16133–16142 (June 2023)
33. Yun, S., Han, D., Oh, S.J., Chun, S., Choe, J., Yoo, Y.: Cutmix: Regularization strategy to train strong classifiers with localizable features. In: Proceedings of the IEEE/CVF international conference on computer vision. pp. 6023–6032 (2019)
34. Zhang, H., Cisse, M., Dauphin, Y.N., Lopez-Paz, D.: mixup: Beyond empirical risk minimization. arXiv preprint arXiv:1710.09412 (2017)

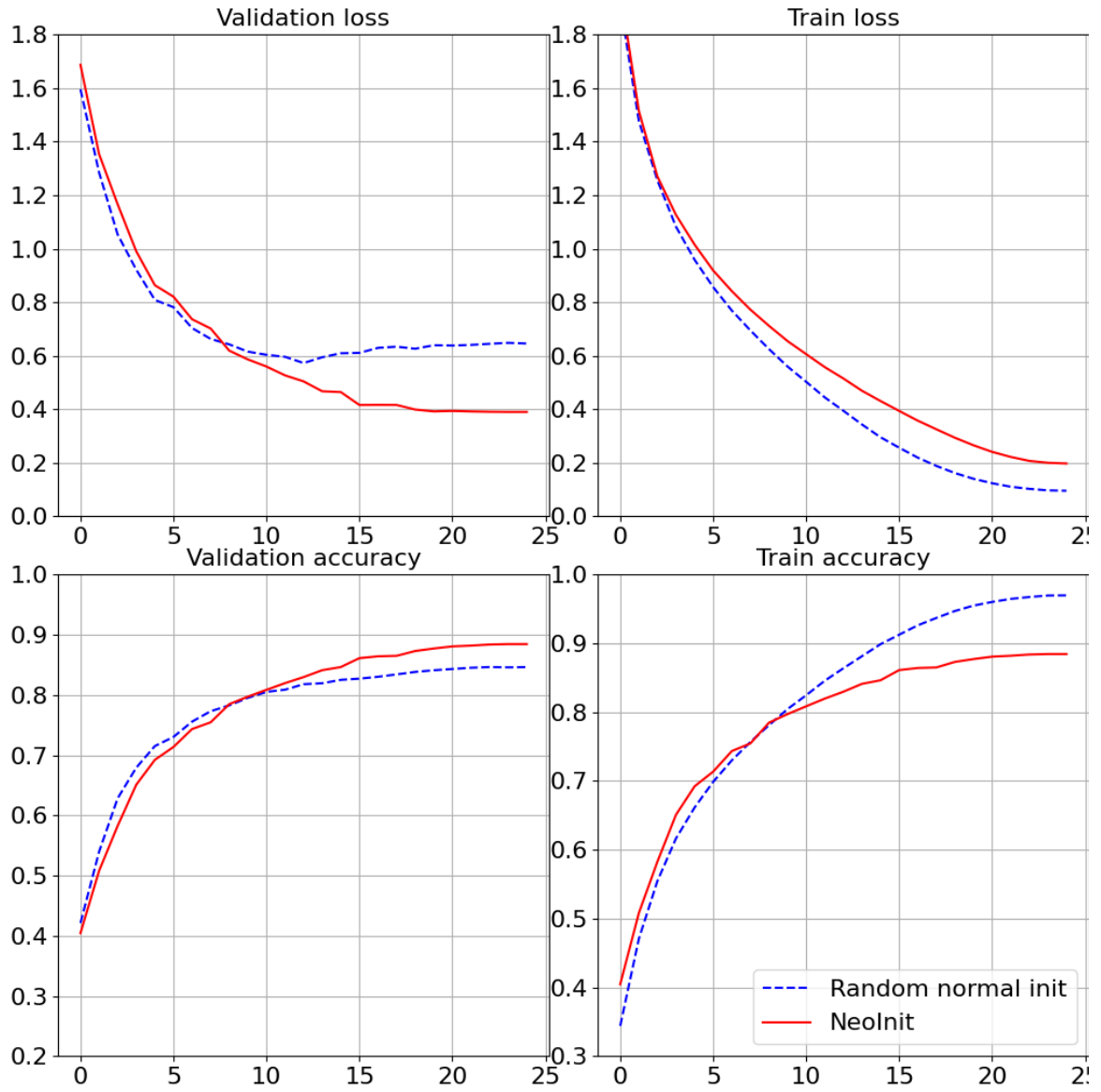


Fig. 6: NeoInit CIFAR-10 ablation experiments